Step Change Detection Based on Analytic Signal for PMU Calibrators

Marcelo Britto Martins
DIMCI
INMETRO
Duque de Caxias, Brazil
mbmartins@inmetro.gov.br

Renata T. de Barros e Vasconcellos
DIMCI
INMETRO
Duque de Caxias, Brazil
rbvasconcellos@inmetro.gov.br

Paulo A. A. Esquef
COMAC
Nat. Lab. for Scientific Computing (LNCC)
Petrópolis, Brazil
pesquef@lncc.br

***Abstract*—The proper tackling of rapid transients, such as voltage sags and swells, by protection systems of power grids that increasingly incorporate low-inertia renewable generators is a current concern in the power generation and metrology communities. In a previous paper, we have reported the characterization of a PMU calibration system that handles synchronized generation and sampling of signals with magnitude and phase step discontinuities. That calibrator employed an iterative parametric method that estimates the underlying phasor parameters, given a priori knowledge of the step location and an initial rough estimate of the phasor frequency. In this paper, we tackle the latter two problems and propose a method that blindly detects a step change from the phasor waveform and provides an accurate estimate of its location in time. Moreover, a simple method that yields a crude estimate of the phasor frequency is also proposed. We measured the accuracy of the estimates in simulated scenarios, including noisy signals.**

***Index Terms*—calibration, frequency, estimation, PMU, sag, step**

I. Introduction

PMUs (Phasor Measurement Units) are devices intended to estimate power system phasors with respect to a reference phasor function, time-synchronous with the UTC, and to report their frequency and rate of change of frequency (ROCOF) at specific timestamps, as defined in the IEEE Standard C37-118.1 [1] (hereafter called IEEE Std). A phasor is a well defined representation of a purely sinusoidal function. The traditional approach for estimating a phasor disrupted by fast transient events is to detect their occurrence and consider the measurements not reliable for the duration of the transient [2]. Recent works propose step-change detection with wavelets [3] and empirical mode decomposition [4]. Reports of severe failures of low-inertia renewable power plants submitted to short duration voltage sags [5], [6] show that protection systems based on PMUs reacted unnecessarily to magnitude and phase steps interfering on the frequency estimation. The authors in [7] are in favor of changing the classical definitions for frequency measurements under step conditions, in order to allow proper separation of low and fast components of the estimated frequency.

In the last years, PMU calibration systems have been developed by National Metrology Institutes (NMIs) [8]–[12], in order to establish metrological infrastructure compliant with the IEEE Std. All of them synchronously generate and sample standardized signals and, for each prescribed test, use specific algorithms to estimate the reference values from the sampled signals. Special effort was spent on the development of dynamic tests [13]–[15], as well as on establishing desired accuracy limits for calibrators [16]. For the specific case of magnitude- and phase-step tests, the *a priori* knowledge of the step location inside a frame is needed as an input to the analysis algorithms. As with the other phasor-related quantities, the reference location should be estimated from samples of the generated signal.

We have recently developed a PMU calibration system meant to reproduce the magnitude- and phase-step tests prescribed in the IEEE Std. A detailed metrological assessment of the aforementioned system is reported in [17]. The parametric estimation we used in [17] featured models that represent separately a single step discontinuity, either in magnitude or in phase, in an observation window. For this, we used the Levenberg—Marquardt iteration (LMI), providing the phasor waveform, a reliable estimate of the step location, and the phasor frequency as known inputs. For locating the step in time we used a detector based solely on the instantaneous *frequency* of Hilbert's analytic signal, which works well for most cases. We have experimentally verified that the detector of [17] tends to miss steps when they occur near a zero-crossing of the observed phasor waveform, a situation that is aggravated as the SNR decreases.

In this paper, we report a deeper investigation on the problem of step change detection and location, as well as, that of obtaining a crude initial estimate of the phasor frequency to feed the LMI. We now formally define (section II-B) and report the accuracy performance (section III) of:

1) a hybrid detector for step-like transients, which is based on the instantaneous *magnitude* and frequency of Hilbert's analytic signal;
2) a simple estimator of the underlying phasor frequency from the instantaneous frequency of Hilbert's analytic signal.

II. Mathematical Background

A. Instantaneous magnitude, phase and frequency

Given a narrowband monocomponent signal $x(t)$, $t \in \mathbb{R}$ let its associated analytic signal be

$$z(t) = x(t) + jH\{x(t)\} = a_i(t)e^{j\theta_i(t)}, \tag{1}$$

where

$$H\{x(t)\} = \int_{-\infty}^{+\infty} \frac{x(u)}{\pi(t-u)}du \tag{2}$$

is the Hilbert Transform of $x(t)$, and the subscript i refers to instantaneous. The instantaneous frequency of $z(t)$ is

$$f_i(t) = \frac{1}{2\pi}\frac{d\theta_i(t)}{dt}. \tag{3}$$

A discrete-time version of $H(x[n])$ can be obtained via the fast Fourier transform [18], from which discrete-time estimates of the instantaneous magnitude $a_i[n]$, phase $\theta_i[n]$ and frequency $f_i[n]$ can be obtained. Discontinuities in the signal can be detected by monitoring anomalies in $a_i[n]$ and $f_i[n]$ [17], [19], [20], by defining appropriate detection signals and threshold levels.

B. Detection of Step-like Transients

Let $x(t)$ be a signal described by the parametric model

$$\begin{aligned} x(t) = & X_m[1+k_x u(t-\tau)]\cos\left(2\pi f_u t + \phi_0 + k_a u(t-\tau)\right) \\ & + \eta(t), \end{aligned} \tag{4}$$

where X_m is the initial magnitude, k_x is the percentage of the magnitude step with respect to X_m, f_u is the underlying frequency, ϕ_0 is the initial phase, k_a is the amplitude of the phase step, $\eta(t)$ is a realization of random process with a given probability density function to represent noise interference, and with $u(t)$ being the unit step function that represents step transitions at the instant $t = \tau$.

For a zero-mean Gaussian white noise, given the standard deviation of the signal $x(t)$, σ_x, and a prescribed SNR level in decibels, the variance of $\eta(t)$ is

$$\eta_0 = \left(\frac{\sigma_x}{10^{\frac{\text{SNR}}{20}}}\right)^2. \tag{5}$$

Let $x[n]$ be a discrete-time ($n \in \mathbb{Z}$) signal obtained by sampling $x(t)$ at $t = n\Delta t$, with Δt the sampling period. The discrete-time version of the analytic signal associated with $x[n]$ is given by [1]

$$z[n] = x[n] + jH\{x[n]\} = a_i[n]e^{j\theta_i[n]}. \tag{6}$$

[1]In the IEEE Std, the letter n denotes the frame index. Here, it denotes sample index within one particular frame.

1) Step detection via instantaneous magnitude: From the first order difference signal $h_i[n] = a_i[n] - a_i[n-1]$, let the detection signal based on the instantaneous *magnitude* be

$$d_{\text{m}}[n] = |h_i[n] - \mathfrak{M}(h_i[n])|, \tag{7}$$

where $\mathfrak{M}(\cdot)$ is the median operator. Given a threshold $\Lambda_{\text{m}} = k_{\text{m}}\mathfrak{M}(d_{\text{m}}[n])$, where k_{m} is a given constant value, the location of a single step in $a_i[n]$ can be estimated as follows. Define the set $\mathcal{N}_{\text{m}} = \{n, d_{\text{m}}[n] \geq \Lambda_m\}$ and let $d_{\text{mmax}} = ||d_{\text{m}}[n]||_\infty$ be the infinity norm of the detection sequence. The index of the magnitude-step is $\hat{n}_{\text{m}} = \{n \in \mathcal{N}_{\text{m}}, d_{\text{m}}[n] = d_{\text{mmax}}\}$. Then, the estimated instant of the step is $\hat{\tau}_{\text{m}} = \hat{n}_{\text{m}}\Delta t$.

2) Step detection via instantaneous frequency: With the discrete-time signal $f_i[n]$ obtained by numerical differentiation of $\theta_i[n]$, we follow the previous notations and define a detection signal based on the instantaneous frequency as [2]

$$d_{\text{f}}[n] = |f_i[n] - \mathfrak{M}(f_i[n])|. \tag{8}$$

Given a threshold $\Lambda_{\text{f}} = k_{\text{f}}\mathfrak{M}(d_{\text{f}}[n])$, where k_{f} is a given constant value, define the set $\mathcal{N}_{\text{f}} = \{n, d_{\text{f}}[n] \geq \Lambda_{\text{f}}\}$ and let $d_{\text{fmáx}} = ||d_{\text{f}}[n]||_\infty$. The index of the magnitude-step is $\hat{n}_{\text{f}} = \{n \in \mathcal{N}_{\text{f}}, d_{\text{f}}[n] = d_{\text{fmax}}\}$ and the corresponding instant is $\hat{\tau}_{\text{f}} = \hat{n}_{\text{f}}\Delta t$.

3) Hybrid Detector: Although both detectors described in sections II-B1 and II-B2 work for either magnitude or phase steps, the former performs better for magnitude steps, whereas the later does a better job in detecting phase steps.

In order to take advantage of both detectors, regardless of the step type, we propose our hybrid step detector, which works as follows:

1) Run the magnitude step detector (II.B.1) to obtain the candidate index $\hat{n}_{\text{m}}$;
2) Run the frequency step detector (II.B.2) to obtain the candidate index $\hat{n}_{\text{f}}$;
3) Calculate the ratios $d_{\text{mmax}}/\Lambda_{\text{m}}$ and $d_{\text{fmax}}/\Lambda_{\text{f}}$;
4) Choose from $\{\hat{n}_{\text{f}}, \hat{n}_{\text{f}}\}$ the index that corresponds to the highest ratio calculated in 3). This index $\hat{n}$ is the final estimate of the step location, with corresponding time instant estimate $\hat{\tau} = \hat{n}\Delta t$.

The hybrid detector can be used when steps happen simultaneously in magnitude and phase or one does not know a priori whether the step happens in magnitude or phase.

4) Frequency estimation: Step changes both in the phasor magnitude or phase are likely to yield spikes in $f_i[n]$. Moreover, it is well known in the literature that the median operator is effective in mitigating the influence of outliers on estimation of mean values. Therefore, the underlying frequency of a signal described by eq. (4) can be estimated as

$$\hat{f}_u = \mathfrak{M}(f_i[n]), \tag{9}$$

where it is assumed that the values of $f_i[n]$ are in Hz.

[2]The expression corresponds to the detector we used in [17].

III. Numeric Simulations

In order to assess the accuracy of the estimators under noisy conditions, we ran Monte Carlo simulations. For each Monte Carlo run, we have digitally generated one frame with 480 samples from equation (4), with $\Delta t = 1/4800$ s, fundamental frequency $f_u = 60$ Hz. Figure 1 shows an example of a sampled signal with a magnitude step near a zero crossing.

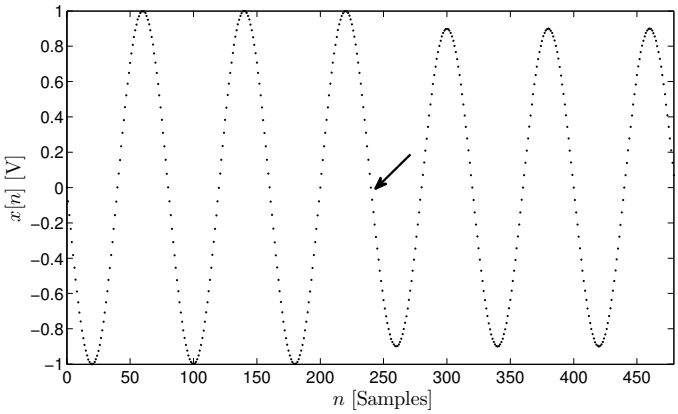

Fig. 1. Sampled signal with magnitude step ($k_x = -0.1, \tau = 240\Delta t$). The arrow indicates a magnitude step near a zero crossing.

A. Performance Metrics

The τ estimation errors are given by

$$\epsilon_\tau = |\hat{\tau} - \tau|, \tag{10}$$

where $\hat{\tau}$ and τ are, respectively, the estimated and reference values. From the set of N_{MC} Monte Carlo runs, with the phasor waveform always containing a step, we define N_{fp} as the number of false positives, i.e., when $\mathcal{N}_{\text{m or f}} \neq \emptyset$, but $\epsilon_\tau > 2\Delta t$, and N_{fn} as the number of false negatives, i.e., when $\mathcal{N}_{\text{m or f}} = \emptyset$. We report the percentage of total failures, i.e.,

$$\mathcal{E}_{\text{f}} = \frac{N_{\text{fp}} + N_{\text{fn}}}{N_{\text{MC}}} \times 100. \tag{11}$$

The frequency errors are calculated by

$$FE = \hat{f}_u - f_u, \tag{12}$$

where $\hat{f}_u$ and f_u are, respectively, the estimated and reference values of the underlying phasor frequency. In Section III-C, we report the mean and standard deviation over the set of N_{MC} estimates of FE.

B. Performance of Step Location

1) Experimental Setup: We have evaluated the performance of the hybrid detector described in (II-B3), with $k_{\text{m}} = k_{\text{f}} = 3$, for the following 3 cases:

1) a single *magnitude*-step ($k_x = -10\%$ and $k_a = 0°$;
2) a single *phase*-step ($k_x = 0\%$ and $k_a = 10°$);
3) and two simultaneous steps occurring in both magnitude and phase ($k_x = -10\%$ and $k_a = 10°$).

For all tests, we set $\tau = 240\Delta t$. To assess the influence on the performance by the relative distance of a step to a zero-crossing of the phasor waveform, we changed the initial phase $\phi_0 \in \{0°, 15°, 30°, 45°, 60°, 75°, 90°\}$ in the model of (4). For our particular choice of τ, a step happens near a zero-crossing when $\phi_0 = 90°$, whereas near the crest of the waveform when $\phi_0 = 0°$. We also evaluated the influence of noise interference on the performance by changing the variance of $\eta(t)$ so to enforce SNRs from 30 to 60 dB (in steps of 10 dB).

2) Results: For each of the setups given in the previous section, the results shown in this section refer to Monte Carlo run with $N_{MC} = 10000$ realizations. The mean performance indicators for the detector II-B3 are organized in Tables I, II, and III.

As can be seen from Table I, the step location performance for case 1 decreases (high $\mathcal{E}_{\text{f}}$) as the SNR decreases, as expected, but increases as ϕ_0 decreases, i.e., as the step gets farther from a zero-crossing. The performance for case 2 (Table II) also decreases with SNR, but increases as ϕ_0 increases, i.e., as the step gets near a zero-crossing.

We observe from Table III that the hybrid detector performs way better for the simultaneous step changes (case 3), this makes sense, since it selects the most reliable estimates of step location from the primary detectors (II-B1 and II-B2). As expected, the performance of the hybrid detector decreases with SNR and when ϕ_0 gets far from $45°$, i.e., the worst cases of the primary detectors.

We have considered as acceptable a 95.45%[3] confidence level for the measure (11). Therefore, all results shown in Table I, II, and III with values below 4.55% are acceptable, e.g., all results for $SNR = 60$ dB, for the 3 tested cases. For $SNR \leq 60$ dB, the reliability of the estimate depends on the specific ϕ_0 value and on the noise level.

As regards the influence of the step height on the performance, we can say that, for $|k_x| > 10\%$ and $10° < |k_a| < 180°$ the performance will be improved in relation to those figures reported in this section. Of course, the performance of the three detectors degenerates as the height of the steps decreases toward zero.

Given Eqs. (7) and (8), and assuming that the samples of those detection signals are normally distributed, corrupted with a few outliers, by choosing $k_{\text{m}} = k_{\text{f}} = 3$ to set the related thresholds, we are considering as outliers samples of $d_{\text{m or f}}[n]$ whose magnitudes are above about two standard deviations [21]. The Gaussianity hypothesis was verified experimentally. Increasing (decreasing) the values of k_{m} and k_{f} tends to increase false negatives (positives). Nonetheless, for $SNR \geq 50$ dB, similar performance figures have been found for $k_{\text{m or f}} \in \{2, 3, 4\}$, revealing that the detector's performance has low sensitivity to the choice of these parameters.

For values of τ set within the range from 5% to 95% of the duration of the frame, we found performance figures similar to those shown in Tables I, II, and III.

[3]For a normal distribution, with a factor of coverage two, as typically considered in metrology.

C. Frequency Estimation

We tested the performance of our proposed phasor frequency estimator (see Section II-B4) for the same 3 cases defined before.

For each case above, we added zero-mean white Gaussian noise to the waveforms, so to enforce SNR levels from 30 dB to 60 dB, in steps of 10 dB. Moreover, we set $N_{\text{MC}} = 10000$ for each Monte Carlo run. Furthermore, ϕ_0 is drawn from a uniform distribution ranging from $0°$ to $90°$. We report the frequency estimation results in terms of mean values and standard deviations, over the set of N_{MC} estimates of FE, as shown in tables VI, IV, and V.

For the case 1, standard deviations of FE for SNR $= 60$ dB are in the order of 0.3 mHz/Hz, in contrast with those in the order of $10\,\mu$Hz/Hz, offered by the much more costly iterative method presented in [17]. Also, there is a significant bias as indicated by the median values. Nevertheless, this crude estimate can serve as an initial guess for the LMI.

IV. Measurements

A. Laboratory setup

A block diagram of the PMU calibration system under development at INMETRO is shown in Figure 2. The hardware architecture is based on a PXI modular system, with capabilities for synchronized generation and sampling of low voltage signals ($< 10\ V_p$). Timing signals from an Atomic Clock are used by the Timing module to discipline trigger and clock for the generation and sampling cards. An external voltage amplifier is used to rise the signal levels to the typical $70\ V_p$ for the input of the Device Under Test (DUT). A resistive voltage divider (RVD) is used to attenuate the signals to $0.8\ V_p$ for the input of the Sampler. The process is controlled by the CPU module, where the reference waveforms are digitally prescribed to be then reproduced by the Generation module. The samples from the Sampling module are read by the CPU, where appropriate algorithms can be implemented to calculate reference values for the calibration of the DUT. For the investigation related in this paper, we use the estimators described in the previous sections to estimate τ and f_u.

Preliminary investigations on the noise conditions show that, depending on the mounting and operation setups, SNRs can be typically within 50 dB to 60 dB, similar to our previous system [17].

B. Performed tests

For a preliminary investigation, we connected the analog output of the Generation module directly to the analog input of the Sampling module, as to eliminate the influence of the Voltage Amplifier and the RVD. Then, we programmed the system to synchronously generate and sample signals of $1V_{\text{rms}}$, all with steps occurring at $\tau = 240\Delta t$, and $f_u = 60$ Hz. After, we tested the step detection and frequency estimation for the worst cases of the 3 tests specified in Section III-B, i.e., case 1 with $\phi_0 = 90°$ and cases 2&3 with $\phi_0 = 0°$.

We made three different measurements, one signal for each case, during which only the intrinsic noise of the system was

TABLE I
PERFORMANCE OF II-B3 – CASE 1.

	Mean $\mathcal{E}_{\text{f}}$ (%)			
	SNR (dB)			
$\phi_0(°)$	60	50	40	30
0	0.0	0.0	0.0	41.4
15	0.0	0.0	0.0	40.6
30	0.0	0.0	0.0	49.5
45	0.0	0.0	0.0	67.9
60	0.0	0.0	1.2	87.1
75	0.0	0.0	34.3	96.8
90	0.0	14.8	91.4	98.9

TABLE II
PERFORMANCE OF II-B3 – CASE 2.

	Mean $\mathcal{E}_{\text{f}}$ (%)			
	SNR (dB)			
$\phi_0(°)$	60	50	40	30
0	0.0	0.2	56.8	97.3
15	0.0	0.0	0.3	84.3
30	0.0	0.0	0.0	43.5
45	0.0	0.0	0.0	13.8
60	0.0	0.0	0.0	5.2
75	0.0	0.0	0.0	3.6
90	0.0	0.0	0.0	2.7

TABLE III
PERFORMANCE OF II-B3 – CASE 3.

	Mean $\mathcal{E}_{\text{f}}$ (%)			
	SNR (dB)			
$\phi_0(°)$	60	50	40	30
0	0.0	0.0	0.0	29.2
15	0.0	0.0	0.0	3.5
30	0.0	0.0	0.0	0.5
45	0.0	0.0	0.0	0.3
60	0.0	0.0	0.0	1.4
75	0.0	0.0	0.01	4.3
90	0.0	0.0	0.0	6.0

TABLE IV
PERFORMANCE OF THE FREQUENCY ESTIMATOR FOR CASE 1.

SNR (dB)	60	50	40	30
Mean FE (mHz/Hz)	-0.24	-0.39	-0.48	-0.50
σ_{FE} (mHz/Hz)	0.32	0.77	2.3	7.1

TABLE V
PERFORMANCE OF THE FREQUENCY ESTIMATOR FOR CASE 2.

SNR (dB)	60	50	40	30
Mean FE (mHz/Hz)	0.92	1.6	2.4	3.4
σ_{FE} (mHz/Hz)	0.51	1.0	2.6	7.2

TABLE VI
PERFORMANCE OF THE FREQUENCY ESTIMATOR FOR CASE 3.

SNR (dB)	60	50	40	30
Mean FE (mHz/Hz)	0.47	0.88	1.5	2.5
σ_{FE} (mHz/Hz)	0.37	0.83	2.4	7.3

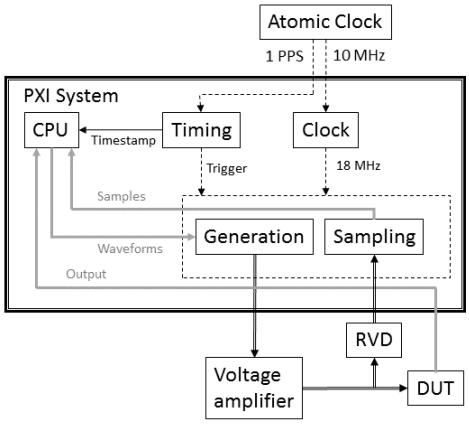

Fig. 2. Block diagram of the current INMETRO's PMU calibration system.

TABLE VII
STEP LOCATION AND FREQUENCY MEASUREMENTS.

Case	ϵ_τ $[\Delta t]$	FE [mHz/Hz]
1	1	-0.44
2	0	0.70
3	1	0.95

present ($\eta_0 = 0$). We report in Table VII the estimation errors for the step instant and phasor frequency. For the cases above, we can say that the contribution of the the hybrid detector to the uncertainty of the ϵ_τ measurements is $\pm 2\Delta t$, with a 95.45% confidence level. For a future complete metrological characterization of the ϵ_τ measurements, we need to consider other error sources in the uncertainty budget. The frequency errors are consistent with the bias and uncertainty reported in section III-C. A further investigation on what is causing the bias on frequency estimates may lead to a proper systematic correction of their values.

V. CONCLUSION

The metrological assessment of PMUs demands systems and methods that must provide accurate reference phasor estimates under dynamic conditions, such as phasor featuring steps in magnitude and phase.

We presented a method that blindly detects and locates step changes from a digitized signal, as well as a simple estimator for the underlying phasor frequency under step conditions. To assess their accuracy limits, we run an uncertainty analysis under different SNR levels by means of Monte Carlo simulations. Additionally, we tested the proposed methods in the PMU calibration system under development at INMETRO, and report preliminary results that seem in agreement with the simulations.

The tests we run so far feature only one step. We plan to extend the detector to estimate the duration of voltage sags, which often last a few cycles and may yield two or more steps inside an observation window. Another front of investigation is to check whether the accuracy of phasor frequency estimates can be increased by means of waveform denoising techniques.

REFERENCES

[1] IEEE, "IEEE standard for synchrophasor measurements for power systems," *IEEE Std C37.118.1-2011 (Revision of IEEE Std C37.118-2005)*, pp. 1–61, Dec 2011.

[2] A. G. Phadke and J. S. Thorp, *Synchronized phasor measurements and their applications*. Springer Science & Business Media, 2008.

[3] J. Barros, M. de Apráiz, and R. I. Diego, "A wavelet-based transient detector for p and m class phasor measurement unit integration," in *2017 IEEE International Workshop on Applied Measurements for Power Systems (AMPS)*, Sept 2017, pp. 1–6.

[4] S. S. Negi, N. Kishor, K. Uhlen, and R. Negi, "Post-processing algorithm for damped and step-change events detection in pmus signal," in *2017 IEEE Manchester PowerTech*, June 2017, pp. 1–6.

[5] P. S. Wright, P. N. Davis, K. Johnstone, G. Rietveld, and A. J. Roscoe, "Field measurement of frequency and rocof in the presence of phase steps," *IEEE Transactions on Instrumentation and Measurement*, vol. 68, no. 6, pp. 1688–1695, June 2019.

[6] A. J. Roscoe, A. Dyśko, B. Marshall, M. Lee, H. Kirkham, and G. Rietveld, "The case for redefinition of frequency and ROCOF to account for ac power system phase steps," in *2017 IEEE Intl. Workshop on App. Meas. for Power Systems (AMPS)*, Sept 2017, pp. 1–6.

[7] H. Kirkham, W. Dickerson, and A. Phadke, "Defining power system frequency," in *2018 IEEE Power Energy Society General Meeting (PESGM)*, Aug 2018, pp. 1–5.

[8] Y.-h. Tang, G. N. Stenbakken, and A. Goldstein, "Calibration of phasor measurement unit at NIST," *IEEE Transactions on Instrumentation and Measurement*, vol. 62, no. 6, pp. 1417–1422, 2013.

[9] J.-P. Braun, C. Mester, and M.-O. André, "Requirements for an advanced PMU calibrator," in *Precision Electromagnetic Measurements (CPEM 2016), 2016 Conference on*. IEEE, 2016, pp. 1–2.

[10] G. Frigo, D. Colangelo, A. Derviškadić, M. Pignati, C. Narduzzi, and M. Paolone, "Definition of accurate reference synchrophasors for static and dynamic characterization of PMUs," *IEEE Trans. on Instr. and Measurement*, vol. 66, no. 9, pp. 2233–2246, Sept 2017.

[11] D. Georgakopoulos and S. Quigg, "Precision measurement system for the calibration of phasor measurement units," *IEEE Trans. on Instr. and Measurement*, vol. 66, no. 6, pp. 1441–1445, June 2017.

[12] S. Svensson, C. Rieck, G. Bideberg, and B. Larsson, "A PMU calibration system," in *Conference on Precision Electromagnetic Measurements*. Paris: IEEE, 2018.

[13] J. Ren, M. Kezunovic, and G. Stenbakken, "Dynamic characterization of PMUs using step signals," in *2009 IEEE Power & Energy Society General Meeting*. IEEE, 2009, pp. 1–6.

[14] G. N. Stenbakken, "Calculating combined amplitude and phase modulated power signal parameters," in *2011 IEEE Power and Energy Society General Meeting*. IEEE, 2011, pp. 1–7.

[15] G. A. Kyriazis, W. G. K. Ihlenfeld, and R. P. Landim, "Estimating parameters of combined AM and PM signals using prior information," *IEEE Transactions on Instrumentation and Measurement*, vol. 64, no. 6, pp. 1760–1766, 2015.

[16] D. Colangelo, L. Zanni, M. Pignati, P. Romano, M. Paolone, J.-P. Braun, and L.-G. Bernier, "Architecture and characterization of a calibrator for PMUs operating in power distribution systems," in *PowerTech, 2015 IEEE Eindhoven*. IEEE, 2015, pp. 1–6.

[17] M. B. Martins, R. T. de Barros e Vasconcellos, and P. A. A. Esquef, "Models for synchrophasor with step discontinuities in magnitude and phase: Estimation and performance," *IEEE Transactions on Instrumentation and Measurement*, pp. 1–8, 2019.

[18] L. Marple, "Computing the discrete-time "analytic" signal via FFT," *IEEE Trans. on Signal Processing*, vol. 47, no. 9, pp. 2600–2603, Sept 1999.

[19] M. Caciotta, S. Giarnetti, F. Leccese, and Z. Leonowicz, "Detection of short transients and interruptions using the Hilbert transform," in *Proc. World Congr. Fundam. Appl. Metrol.*, 2009, pp. 913–916.

[20] P. A. A. Esquef, J. A. Apolinário, and L. W. P. Biscainho, "Edit detection in speech recordings via instantaneous electric network frequency variations," *IEEE Transactions on Information Forensics and Security*, vol. 9, no. 12, pp. 2314–2326, Dec 2014.

[21] P. J. Rousseeuw and C. Croux, "Alternatives to the median absolute deviation," *Journal of the American Statistical Association*, vol. 88, no. 424, pp. 1273–1283, 1993.